Supporting information

Tailoring the 3D porous structure of conducting PEDOT:PSS gels via ice-templating

Quentin Weinbach,[1] Naoures Hmili,[1] Emma Gottis,[1] Guillaume Fleith,[1] Jérôme Combet,[1]

Vasiliki Papaefthimiou,[2] Vincent Malesys,[3] Emmanuel Denys,[3] Laurent Simon,[3] Marc

Schmutz,[1] Alain Carvalho,[1] Doru Constantin,[1] Laure Biniek[1]*

[1] Université de Strasbourg, CNRS, Institut Charles Sadron UPR22, F-67000 Strasbourg, France
[2] Institut de Chimie et Procédées pour l'Energie, l'Environnement et la Sante (ICPEES),
Université De Strasbourg, CNRS UMR 7515, 25 rue Becquerel, F-67087 Strasbourg Cedex 2,
France
[3] Université de Haute-Alsace, CNRS, Institut de Science des Matériaux de Mulhouse UMR
7361, 3Bis rue Alfred Werner, 68093 Mulhouse, France
*E-mail: laure.biniek@ics-cnrs.unistra.fr

## 1) Direct lyophilization of the PH1000 dispersion
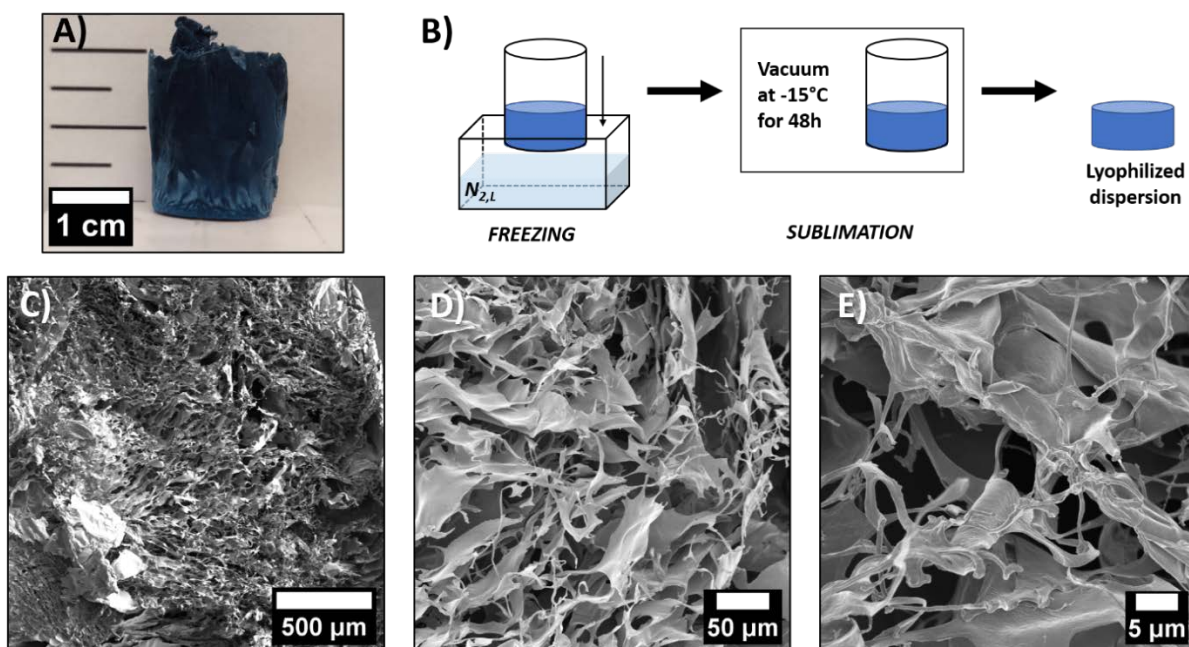
Figure ESI 1: A) Digital photo of the lyophilized PEDOT:PSS dispersion, B) Schematic of the

lyophilization steps, C-D) SEM images at different spots and magnifications of the lyophilized

dispersion.

2) SAXS data on the PH1000 dispersion and TEM on the acidified dispersion
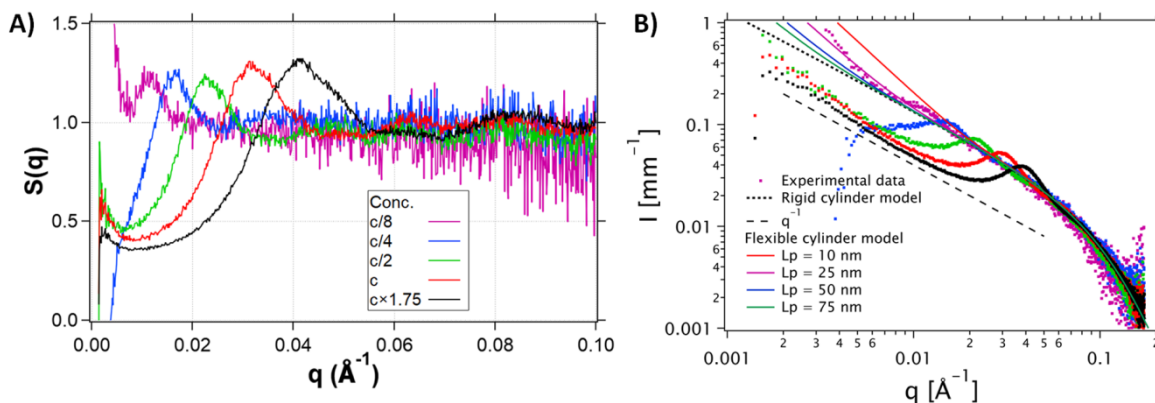
Figure ESI 2: A) Serial dilution of PH1000 dispersion in SAXS, structure factor plotted as a function of the scattering vector (q). S(q)is obtained by dividing the scattered intensity I(q) by the fitted intensity associated to the cylindrical model. B) Scattered intensity I(q) with rigid cylinder model (as in Figure 2.A) and with flexible cylinder models for various persistence length values Lp between 10 and 75 nm (solid colored lines).

## 3) Cryo-TEM on PH1000 dispersion
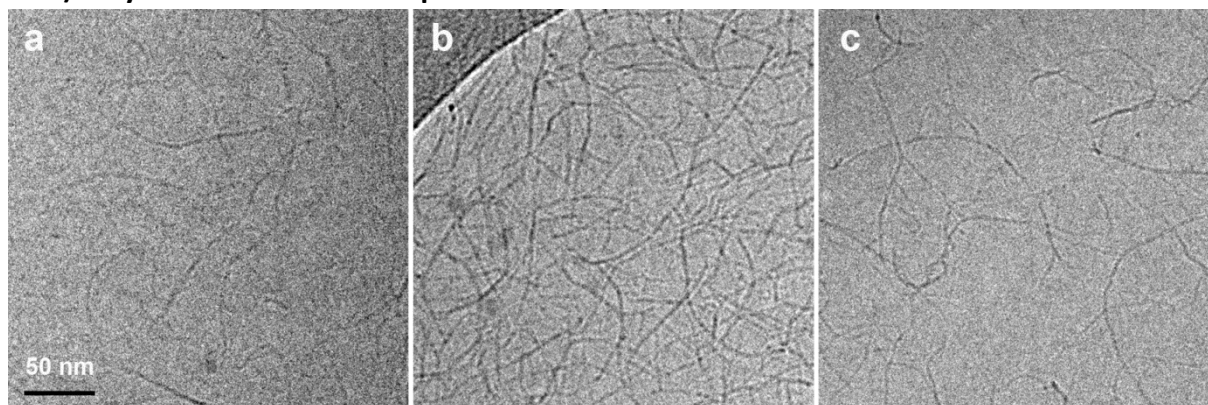
Figure ESI 3: a) Cryo-TEM on PH1000 (Clevios[TM], batch number 9007086839, received and opened October 2022, kindly provided by Fouzia Boulmedais, filtered on 0.45 µm and diluted 8 times. b) cryo-TEM on PH1000 (Clevios[TM], batch number 9007391368, used for all experiments, received in September 2021, opened in November 2021), not filtered, not diluted. c) cryo-TEM on acidified PH1000 dispersion (Clevios[TM], batch number 9007391368) filtered on 0.45 µm, diluted 8 times, acidified and further diluted 10 times). Fibers present entanglements.

Stability of the commercial PEDOT:PSS dispersion was one of our particular concern. For this reason we have performed cryo-TEM studies with several product batches (relatively recent and stored in a dark refrigerator, as recommended by the supplier). We observed a majority of cylinder like objects for all samples, in as-received or diluted or filtered dispersion. Note that both cryo-TEM and SAXS perturb the suspensions much less than the process of drying them onto a grid for classical TEM, so the former techniques are less prone to artifacts than the latter.

### 4) UV-Visible spectroscopy analysis of the gel supernatant
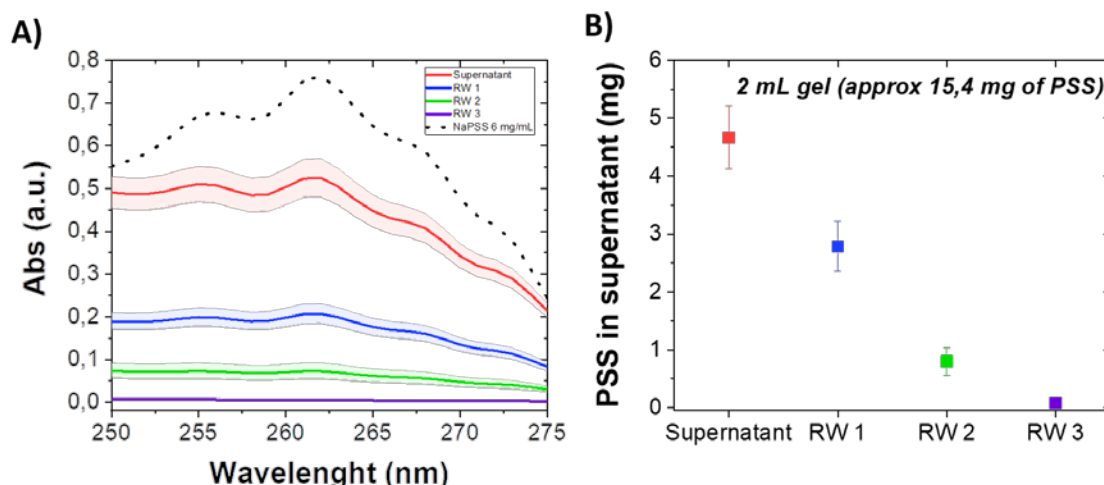
Figure ESI 4: A) UV-Vis spectra of the gel supernatant and the three rinsing water (RW), for reference the UV-Vis spectra of a 6 mg/mL NaPSS solution in deionized water is also plotted (dashed line). B) Estimated PSSH mass found in gel (2 mL) supernatant and the three rinsing water (determined by UV-Vis spectra via the Beer- Lambert law following the peak @ 262 nm and a calibration curve).

With the Beer-Lambert law, it is possible to determine the mass of PSS which is solubilized in the supernatant during the gelation process (~8 mg in 2 mL initial dispersion). The molar extinction coefficient of PSS (1.45×10^{6} L.mol^{-1}.cm^{-1}) was determined using a calibration curve of NaPSS in deionized water. Interestingly, a certain quantity of PSS can be further

washed out from the gel after two rinsing steps in deionized water. A third rinsing step (RW3) appears to be not necessary.

5) SAXS data on the hydrogel
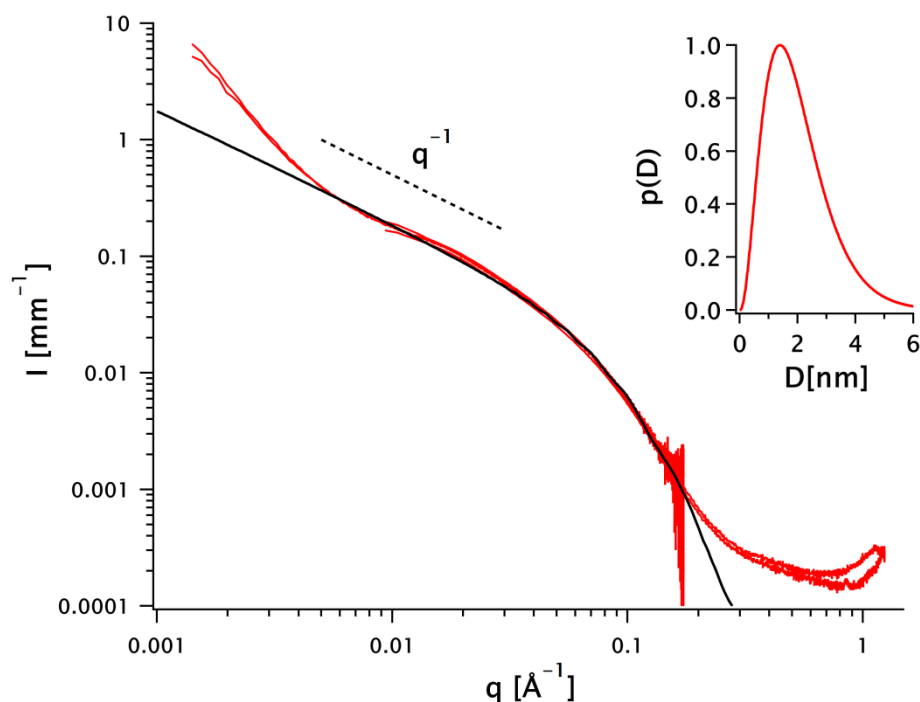
Figure ESI 5: Hydrogel characterization, scattered intensity as a function of the scattering vector, I(q), for the SAXS configurations, in red, and fit with a cylinder model, in black. The diameter polydispersity is described by a Schulz distribution p(D), displayed in the inset.

The cylinder model (in black) implemented by the NIST data analysis library [S. R. Kline, *J. Appl. Crystallogr.* **2006**, *39*, 895.]) yielded a mean fibril diameter D = 2 nm, with a relative polydispersity σ_D/D = 0.55. The model is valid in q range of 0.005 Å^{-1} < q < 0.18 Å^{-1}. At lower-q value (<0.005 Å^{-1}), the deviation from the cylinder model may arise from fibrils interactions.

5) IR spectra of the dried dispersion and dried gel
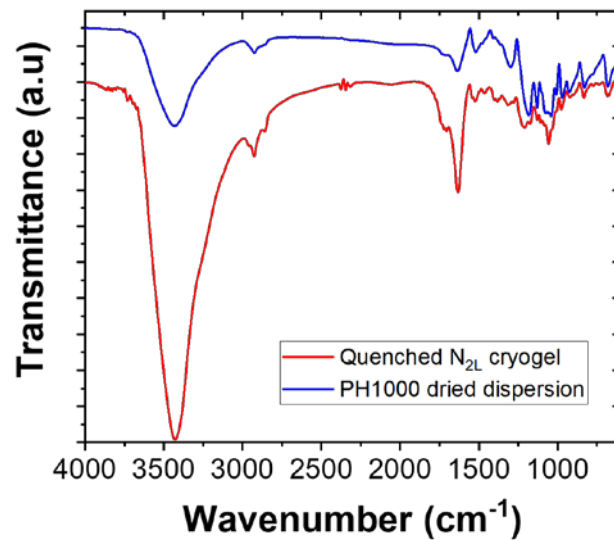
Figure ESI 6: Full FTIR spectra of the quenched N_{2L} cryogel (in red) and the PH1000 dried dispersion (in blue). Both were dispersed in KBr pellets for measurement.

6) Pore walls thickness measurements
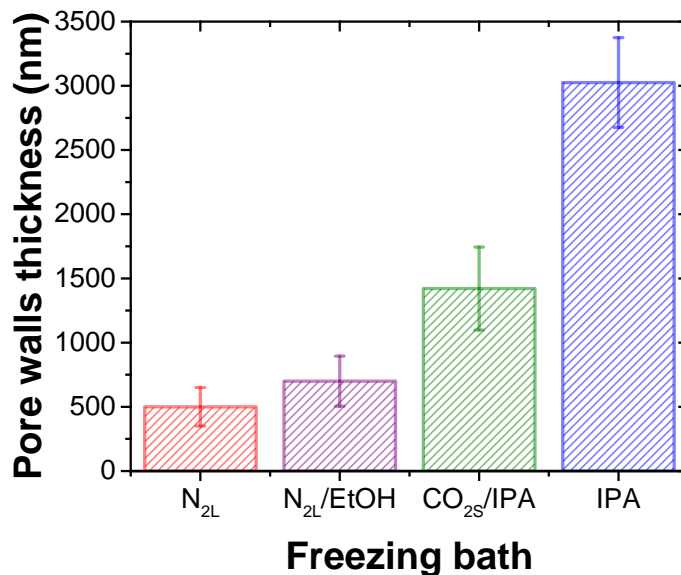
Figure ESI 7: Evolution of pore walls thickness in templated cryogels as a function of the cooling bath nature (and temperature). Cooler the bath, higher the freezing rate, thinner the pore walls.

7) Discussion on electrical conductivity measurements

a) Four-probe collinear method might show limitation when applied to porous structure. To further validate our method, we have used the two-contact resistance measurement with metal plates placed at the top and bottom interface of one cryogel sample (thickness l=0.96 cm and diameter = 1.32 cm). We had to apply a small pressure to enhance the contacts. We found a resistance of 0.75 Ω, providing a conductivity of 0.93 S.cm^{-1} (using the following equation $\sigma = \frac{1}{R} \cdot \frac{l}{A}$, $with\ A\ cross\ section\ area$), in the same range as the one found by the 4-probe collinear method for the templated $N_{2,L}$ cryogel sample. In both methods, the effect of contact resistance should be considered carefully. We believe that our data are confirmed by the agreement of the two methods, but we have ongoing work to maximize the contacts between the metallic probe and porous samples.

b) We made our own reference film by adding sulfuric acid (same concentration than the one use for gelation) to the PEDOT:PSS dispersion, followed by drop casting in a crystallizing dish. The dispersion was left to dry on a hot plate at 100°C for 3 h. The dried film was peeled off with a razor blade, rinsed with distilled water and further dried on a hot plate at 100°C. The electrical conductivity of this reference film (~7 µm thickness) was measured by the four- probe collinear method, yielding a value of 508 $\pm$ 70 S.cm^{-1}.

The difference in electrical conductivity between the reference thick film and the cryogels can be attributed to the high porosity of the latter. The apparent values measured for the cryogel take into account the porosity of the samples.

Empirical equations have been proposed to describe the relationship between porosity and electrical conductivity for metallic foams (Cuevas et *al. J. Porous Mater* 2009, **16**, 675).

Unfortunately, to the best of our knowledge, no modelling of the electrical conductivity of porous conducting polymers can be found in the literature.

Nevertheless, if we consider our porous structure as a closed-cell foam structure (although the cryogel structure is far from this ideal case), we can apply the following equation to estimate σ_{dense} using σ_p (the apparent electrical conductivity) and P (the porosity):

$$\sigma_r = \frac{\sigma_p}{\sigma_d} = (1 - P)^{3/2} = 380 \text{ S.cm}^{-1}$$

The σ_{dense} value estimated from this equation is in the same order of magnitude than the one measured on the reference dense films. This conclusion has been confirmed by mesoscopic measurements of the electrical conductivity (collinear and square geometries), whose value range, at the scale of a single pore wall, is similar to the reference thick film or the σ_{dense} value estimated above. The preliminary results yielded a relatively high dispersion of conductivity values (a few dozens to a few hundred of S.cm^{-1} depending on the considered wall and corresponding thickness, which was not always properly measurable). Further nanoprobing measurements are needed to confirm the absolute value of electrical conductivity at the scale of a pore wall.
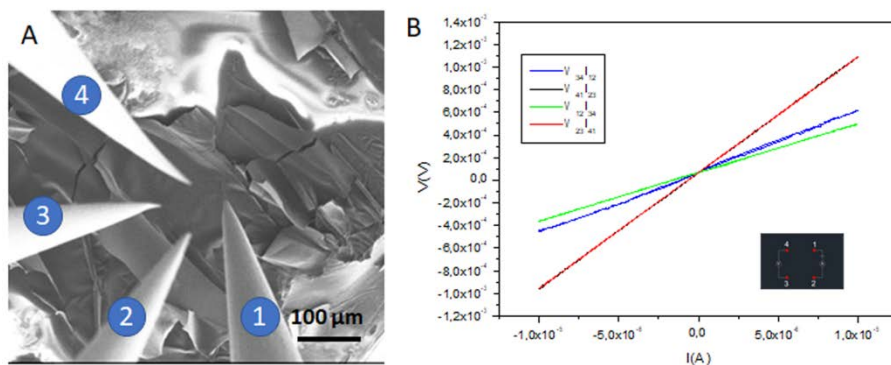
Figure ESI8: Mesoscopic electrical transport measurement on a pore wall of an templated $N_{2,L}$ cryogel. A) SEM image of the four-probes in a square geometry (four-probe resistivity measurements with the van der Pauw method). B) Typical V(I) curves.